THE JOURNAL OF PHYSICAL CHEMISTRY B

Article

pubs.acs.org/JPCB

Pronounced Hydrogen Bonding Giving Rise to Apparent Probe Hyperpolarity in Ionic Liquid Mixtures with 2,2,2-Trifluoroethanol

Shruti Trivedi,[†] Shubha Pandey,[‡] Sheila N. Baker,*[,§] Gary A. Baker,*[,‡] and Siddharth Pandey*[,†,‡]

[†]Department of Chemistry, Indian Institute of Technology Delhi, Hauz Khas, New Delhi −110016, India

[‡]Department of Chemistry, University of Missouri—Columbia, Columbia, Missouri 65211, United States

[§]Department of Chemical Engineering, University of Missouri—Columbia, Columbia, Missouri 65211, United States

ABSTRACT: The fascinating and attractive features of ionic liquids (ILs) can be considerably expanded by mixing with suitable cosolvents, opening their versatility beyond the pure materials. We show here that mixtures of the IL 1-butyl-3-methylimidazolium hexafluorophosphate ([bmim][PF_6]) and 2,2,2-trifluoroethanol (TFE) display the intriguing phenomenon of hyperpolarity, examples of which are notably sparse in the literature. From the perspective of the E_T^N polarity scale and Kamlet−Taft parameters for hydrogen bond acidity (α) and basicity (β), the polarity of this mixture exceeds that of either neat component. Fluorescent molecular probes capable of engaging in hydrogen bonds (e.g., 2-(*p*-toluidino)naphthalene-6-sulfonate, TNS; 6-propionyl-2-(dimethylamino)naphthalene, PRODAN) also exhibit this curious behavior. The choice of IL anion appears to be essential as hyperpolarity is not observed for mixtures of TFE with ILs containing anions other than hexafluorophosphate. The complex solute−solvent and solvent−solvent interactions present in the [bmim][PF_6] + TFE mixture were further elucidated using infrared absorbance, dynamic viscometry, and density measurements. These results are discussed in terms of Coulombic interactions, disruption of TFE multimers, formation of hyperanion preference aggregates, and "free" [bmim]$^+$. It is our intent that these results open the door for computational exploration of related solvent mixtures while inspiring practical questions, such as whether such systems might offer the potential for stabilization of highly charged transition states or ionic clusters during (nano)synthesis.

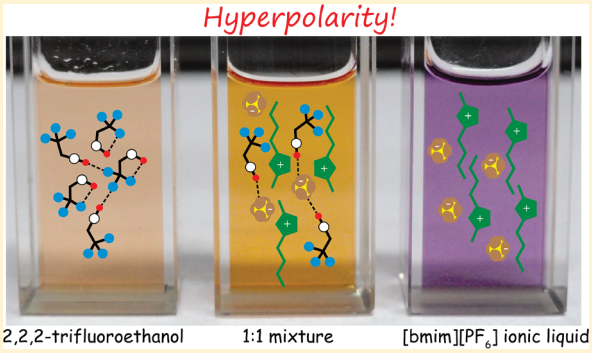

INTRODUCTION

Ionic liquids (ILs) are currently the focus of widespread research due to their diverse ability to serve as novel reaction media, stationary phases in gas chromatography, electrolytes, lubricants, heat-transfer fluids, and so forth.[1−5] The unchecked growth in IL research interest is a direct consequence of the unique composition and tailorable ionic architectures possible for these fluids which yield, at times, seemingly anomalous behavior. The suitable combination of functional constituent ions is responsible for their definitive properties, and this control over their features derives immense benefit for their exploitation in a host of areas. Moreover, ILs constitute an important class of Coulombic fluids whose molecular constituents are complex ions that render their chemistry uniquely different from common molecular solvents or aqueous electrolytes.

Although abundant literature exists on applications of ILs as solvent media for chemical reactions, their potential usage in chemical applications is often hindered by their limited and, in some cases, undesirable physicochemical properties (e.g., high viscosity). Although IL properties may be tuned by altering the cation/anion combination, the extent to which any one key property may be modified is often fairly limited. Consequently, cosolvent-modified IL systems are becoming a topic of active research to explore the extent to which favorably modified properties can be achieved in such mixed systems.[6,7] In this context, judicious selection of cosolvent is key to affording the desired system properties. Further, if one wishes to maintain an intrinsic property of the IL (such as biological compatibility, low volatility, etc.), the selected cosolvent chosen must of course also share these desired properties as well.

Against this backdrop, 2,2,2-trifluoroethanol (TFE), a fluorinated solvent that demonstrates excellent environmental and biological compatibility, was investigated as a cosolvent in the current study. Moreover, from the experimental point of view, TFE is completely miscible with many prevalent ILs, including the imidazolium and pyrrolidinium cation-based ILs used in this investigation. TFE, due to the electronegativity of the trifluoromethyl group, exhibits significantly stronger acidic character as compared to conventional alcohols like ethanol and is known to form stable complexes with heterocycles, such as THF or pyridine, through hydrogen bonding. A consequence of this feature is that the hydrogen bond accepting (HBA) basicity parameter (β) of TFE is close to zero, whereas the

Received: October 24, 2011
Revised: December 30, 2011
Published: January 6, 2012

   dx.doi.org/10.1021/jp210199s | *J. Phys. Chem. B* 2012, 116, 1360−1369

hydrogen bond donating (HBD) acidity (α) of common IL cations is substantial.[8] In general, TFE is found to promote the formation of secondary structure in polypeptides and proteins[9] and can alter the folding/unfolding kinetics of proteins.[10] As a result, it is a widely used cosolvent in biophysical and biotechnological investigations.[11] Due to its physical and chemical properties, TFE is used as a solvent in the electrochemical oxidation of various organic compounds.[12] TFE also has many uses as a solvent in organic chemistry,[13,14] including the oxidation of sulfur compounds using hydrogen peroxide.[15] Finally, TFE has been used for capillary zone electrophoresis peptide separations in aqueous−organic media,[16] as a solvent for nylon, and in the pharmaceutical field.[17]

A few earlier attempts to study IL/TFE mixtures were conducted by different research groups.[18−24] Currás et al. studied the physicochemical properties of binary mixtures of TFE with the ILs 1-butyl-3-methylimidazolium tetrafluoroborate, [bmim][BF_4], and 1-ethyl-3-methylimidazolium tetrafluoroborate, [emim][BF_4], as replacements for classical refrigerant/absorbent pairs and found that the mixtures, based on density measurements, possess excess molar volumes which they attribute to the presence of TFE's fluorine atoms.[23] In another study, TFE and 1-hexyl-3-methylimidazolium chloride, [hmim][Cl], mixtures were used to controllably produce well-defined poly(3-(*N*-2-methacryloyloxyethyl-*N*,*N*-dimethyl)ammonatopropanesulfonate) brushes and the corresponding free polymer with a predictable number-average molecular weight (M_n) from 1×10^4 to 3×10^5 g mol^{-1} and narrow molecular weight distributions of 1.15−1.25.[24] This high level of control was attributed to the affinity of the TFE and [hmim][Cl] for sulfobetaine monomers. IL + TFE combinations were also employed for nucleophilic substitutions of chlorobis(4-methoxyphenyl)methane.[25] Here, the values of the kinetic constants were found to significantly increase upon going from TFE/acetonitrile to TFE/IL mixtures.[25]

In this paper, we report dramatic and unanticipated responses from select solvatochromic probes dissolved in binary mixtures of 1-butyl-3-methylimidazolium hexafluorophosphate with TFE, including the phenomenon of *hyperpolarity* in which the apparent polarity from the perspective of the probe exceeds that experienced in either neat solvent. Our results unveil interesting synergistic interactions present within this mixed solvent system, a postulate supported by Fourier-transform infrared (FTIR), viscometry, and density measurements on IL/TFE mixtures. These interactions appear to impart to these (and related) cosolvent systems favorable physicochemical properties, further expanding the application potential of hybrid IL-based media.

EXPERIMENTAL SECTION

Materials. 2,6-Diphenyl-4-(2,4,6-triphenylpyridinium-1-yl)-phenolate (betaine dye 30) (≥99%), 4-nitroaniline (NA) (≥90%), and *N*,*N*-diethyl-4-nitroaniline (DENA) were purchased from Fluka, Spectrochem Co. Ltd., and Frinton Laboratories, respectively, and recrystallized multiple times before use. The fluorescence probes 2-(*p*-toluidino)-naphthalene-6-sulfonate (TNS), 6-propionyl-2-(dimethylamino)naphthalene (PRODAN), and pyrene (Py) were purchased from Fluka, Acros Organics, and Sigma-Aldrich, respectively, in the highest purity possible. Structures of all probes are presented in Scheme 1. 2,2,2-Trifluoroethanol (TFE) (99.8%) and ethanol (HPLC grade) were purchased

Scheme 1. Chemical Structures of the Polarity-Responsive Probes Used in this Study

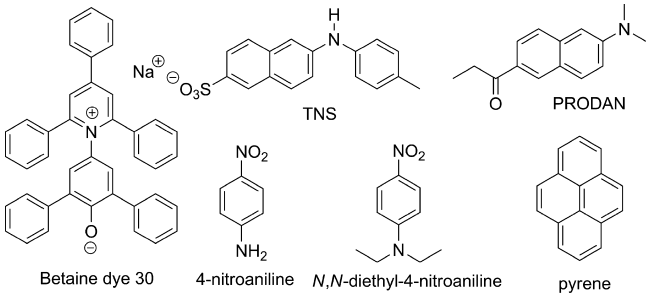

from Acros Organics and Merck, respectively, and were used as received. Spectroscopic-grade high purity ILs 1-butyl-3-methylimidazolium hexafluorophosphate ([bmim][PF_6]), 1-hexyl-3-methylimidazolium hexafluorophosphate ([hmim]-[PF_6]), 1-butyl-3-methylimidazolium tetrafluoroborate ([bmim][BF_4]), 1-hexyl-3-methylimidazolium tetrafluoroborate ([hmim][BF_4]), 1-octyl-3-methylimidazolium tetrafluoroborate ([omim][BF_4]), 1-butyl-3-methylimidazolium bis-(trifluoromethanesulfonyl)imide ([bmim][Tf_2N]), and 1-butyl-1-methylpyrrolidinium tetracyanoborate ([bmpyrr][B-$(CN)_4$] were prepared according to procedures described in the literature.[26,27] Water contents of these ILs were determined using Karl Fischer titration prior to experiments to ensure water contents below100 ppm.

Methods. All absorbance and fluorescence probe stock solutions were prepared in ethanol and stored in ambered glass vials at 4 ± 1 °C. To prepare samples for measurement, the appropriate volume of the probe stock solution was transferred to a clean quartz cuvette and the ethanol removed using a gentle flow of nitrogen. IL + TFE mixtures of desired compositions were prepared by mass and then introduced to the cuvette to achieve the final desired probe concentration.

A Perkin-Elmer Lambda 35 UV−vis double beam spectrophotometer with variable bandwidth was used for acquisition of the UV−vis absorbance data. Fluorescence spectra were acquired on a model FL 3-11 Fluorolog-3 modular spectrofluorometer (Horiba-Jobin Yvon, Inc.) with single Czerny−Turner grating excitation and emission monochromators as wavelength selection devices, a 450 W Xe-arc lamp as the excitation source, and a PMT as the detector. Fluorescence spectra of the probes were collected with the following excitation/emission slit widths (in nm): TNS, 3/3; PRODAN, 1/1; Py, 1/1 under excitation at 320, 350, and 337 nm, respectively. All reported spectroscopic values were averages based on perfoming triplicate measurements on independently prepared samples. The spectral responses from appropriate blanks were subtracted before data analysis in each case. All absorbance and fluorescence data were acquired using 1.0 mm and 10.0 mm path length quartz cuvettes, respectively. Fourier-transform infrared (FTIR) absorbance data were acquired on a Nicolet 6700 FTIR double-beam spectrophotometer. Dynamic viscosities (η) were measured with a Peltier-based (resolution of 0.01 °C and accuracy <0.05 °C) automated Anton Paar microviscometer. The error in η was ≤0.5%. Densities of the IL + TFE mixtures were measured using a Peltier-based Mettler Toledo DE45 delta range density meter. All data analysis was performed using SigmaPlot v11.0 software.

dx.doi.org/10.1021/jp210199s | J. Phys. Chem. B 2012, 116, 1360−1369

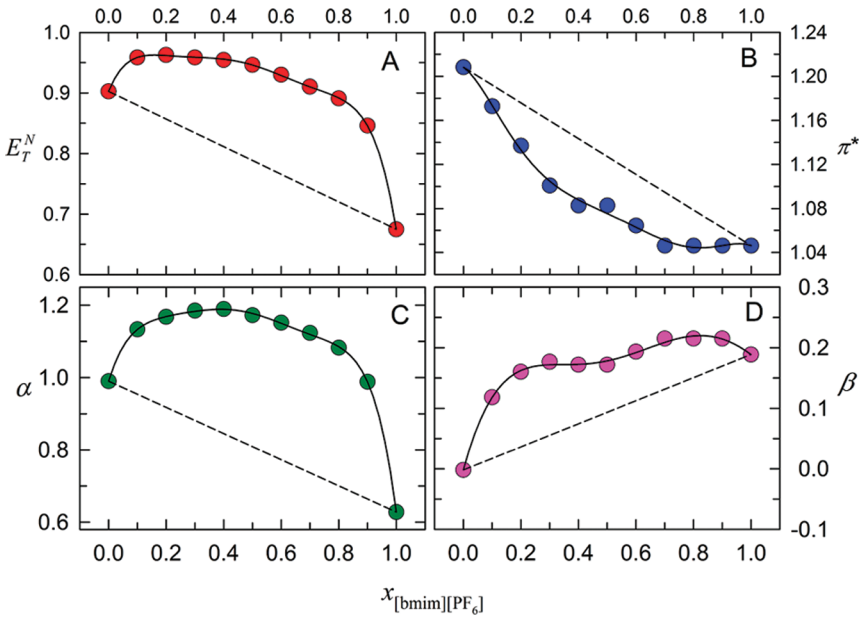

Figure 1. Empirical solvent polarity (A) E_T^N and Kamlet–Taft parameters (B) dipolarity/polarizability (π^*), (C) HBD acidity (α), and (D) HBA basicity (β) determined for the [bmim][PF_6] + TFE system under ambient conditions. Dashed lines represent mole-fraction-weighted (ideal) behavior whereas the solid curves in each panel denote fit results according to a Redlich–Kister expression (eq 7); the associated R–K parameters are given in Table 1.

RESULTS AND DISCUSSION

Behavior of Reichardt's Dye 30 in [bmim][PF_6] + TFE Mixtures. Betaine dye 30, better known as Reichardt's dye, is a popular solvatochromic absorbance probe that exhibits an unusually pronounced band shift in response to changes in solvent polarity.[8] The lowest-energy intramolecular charge-transfer (ICT) absorption band of betaine dye 30 is hypsochromically shifted by some 357 nm in going from the nonpolar solvent diphenyl ether (λ_{max}^{abs} = 810 nm) to the highly polar, protic solvent water (λ_{max}^{abs} = 453 nm), where λ_{max}^{abs} is the wavelength of maximal absorption for the ICT band. The negative solvatochromism of the betaine dye 30 originates from the differential solvation of its highly polar equilibrium ground state and the less polar first Franck–Condon excited state, which becomes more prominent with increasing solvent polarity. There is a considerable charge transfer from the phenolate to the pyridinium moiety of the zwitterionic dye. Thus, Reichardt's dye is strongly affected by both the dipolarity/polarizability (π^*) and the hydrogen bond donor strength (α parameter) of the solvent; i.e., hydrogen-bond donating solvents stabilize the ground state more than the excited state. The well-known empirical scale of solvent polarity, $E_T(30)$, is defined as the molar transition energy of the dye, traditionally expressed in kcal mol^{-1}, at standard temperature and pressure according to the expression $E_T(30)$ = 28 591.5/λ_{max}^{abs} (nm). The $E_T(30)$ values can be subsequently expressed in normalized E_T^N values using the conversion

$$E_T^N = \frac{[E_T(30)_{SOLVENT} - E_T(30)_{TMS}]}{[E_T(30)_{WATER} - E_T(30)_{TMS}]} \quad (1)$$

where TMS is tetramethylsilane. Using $E_T(30)_{WATER}$ = 63.1 kcal mol^{-1} and $E_T(30)_{TMS}$ = 30.7 kcal mol^{-1}, eq 1 can be recast as

$$E_T^N = \frac{[E_T(30)_{SOLVENT} - 30.7]}{32.4} \quad (2)$$

E_T^N is thus dimensionless and varies between 0 for TMS (a very nonpolar solvent) and 1 for water (very polar).

UV–vis absorbance spectra of betaine dye 30 dissolved in [bmim][PF_6] + TFE mixtures over the entire composition range were acquired and the corresponding E_T^N values calculated and summarized in Figure 1A. Our recovered E_T^N values for neat [bmim][PF_6] and TFE are in excellent agreement with those reported in the literature,[19,28] and as expected, the E_T^N value in neat TFE is significantly higher than in neat [bmim][PF_6] due to the higher HBD acidity of TFE. An unanticipated outcome of our measurements is the significantly enhanced E_T^N observed for the [bmim][PF_6] + TFE mixtures. Remarkably, although the E_T^N value for neat TFE far exceeds that in pure [bmim][PF_6], E_T^N becomes higher still as [bmim][PF_6] is added to TFE. This is even the case for a [bmim][PF_6] mole fraction, $x_{[bmim][PF6]}$, of just 0.1. A careful examination of Figure 1A reveals this to be true for all intermediate mole fractions of [bmim][PF_6] below 0.8. For $x_{[bmim][PF6]}$ of 0.8 and higher, the observed E_T^N values are no longer higher than that of neat TFE. The experimental E_T^N values do, however, remain significantly higher than the mole-fraction-weighted (ideal) prediction illustrated by the dashed curve. When such deviations from ideal, arithmetically derived values are observed, preferential solvation is often invoked in explanation. Of course, even in the event of absolute preferential solvation of the probe by TFE, absent other mechanisms, the experimental E_T^N value cannot exceed the value in neat TFE. In this case, this unusually high E_T^N value indicates a mixture possessing greater π^* and/or α character than those of either neat component. We have previously observed this phenomenon of synergistic polarity, an effect we have termed "hyperpolarity", in [bmim][PF_6] + tetraethylene glycol (TEG)

dx.doi.org/10.1021/jp210199s | J. Phys. Chem. B 2012, 116, 1360–1369

and [bmim][PF_6] + poly(ethylene glycol) (PEG) mixtures, but the effect is absent in IL mixtures with common organic solvents including aliphatic alcohols such as ethanol.[27−31] Interestingly, and as discussed further in a later section of this paper, we find this behavior unique to [PF_6]$^-$-based ILs. Thus, it appears that the presence of [PF_6]$^-$ alongside TFE is necessary to induce the synergy in solvation which gives rise to hyperpolarity in E_T^N values within [bmim][PF_6] + TFE mixtures.

Kamlet−Taft Parameters for [bmim][PF_6] + TFE Mixtures. The reason for preferential solvation, in most cases, is the favorable interaction(s) that may exist between the solute and *one* of the solvents (or its components) in the mixture.[32,33] However, as mentioned earlier, preferential solvation alone cannot explain the enhanced synergism of E_T^N within [bmim][PF_6] + TFE mixtures. Therefore, significant changes in solute−solvent and/or solvent−solvent interactions within the mixture are indicated.[32,33] In order to further elucidate this striking observation, we determined the Kamlet−Taft solvatochromic parameters[34−37] (π^*, α, and β) for the binary mixture. Recall that E_T^N values are influenced mostly from π^* and α contributions. The π^* values were estimated from the absorption maxima of *N*,*N*-diethyl-4-nitroaniline (DENA) ($\bar{\nu}_{DENA}$in kK), a non-HBD solute, using the following:

$$\pi^* = 8.649 - 0.314\bar{\nu}_{DENA} \quad (3)$$

The α values were determined from $E_T(30)$ and π^* using[28]

$$\alpha = 0.0649E_T(30) - 2.03 - 0.72\pi^* \quad (4)$$

and β values are estimated from the enhanced solvatochromic shift of 4-nitroaniline (NA) relative to its homomorph DENA by

$$\beta = -0.357\bar{\nu}_{NA} - 1.176\pi^* + 11.12 \quad (5)$$

The π^* values indicate the impact of solvent dipolarity/polarizability on the probe molecule DENA.[38,39] From the UV−vis absorbance spectra of DENA in the different compositions of the [bmim][PF_6] + TFE mixture, π^* was estimated using eq 3 as presented in Figure 1B where ideal π^* values are indicated by the dashed line. Again, similar to E_T^N, the π^* of neat TFE is observed to be higher than that of neat [bmim][PF_6], indicative of the higher dipolarity/polarizability of TFE over [bmim][PF_6]. Our π^* values in neat [bmim][PF_6] and in neat TFE are in good agreement with those reported in the literature.[19,39,40] However, contrary to what was observed for E_T^N, π^* abruptly falls as [bmim][PF_6] is added to TFE. Further, at all compositions of the [bmim][PF_6] + TFE mixture, π^* is always lower than the predicted value. While preferential solvation of DENA by the more polar TFE may be expected, these results clearly indicate that this is not the case. In fact, it appears that DENA is preferentially solvated by [bmim][PF_6], and at $x_{[bmim][PF6]} > 0.7$, DENA is almost exclusively solvated by [bmim][PF_6]. This is in line with a previous report showing DENA is preferentially solvated by ILs in binary IL/organic solvent mixtures until a large mol % of organic solvent is present.[19] These data lend credence to the unusual response of betaine dye 30 in [bmim][PF_6] + TFE as being a consequence of hydrogen bonding (H-bonding) behavior, in particular α, rather than dipolarity/polarizability effects.

To investigate this further, the α values were obtained from $E_T(30)$ and π^* (eq 4), as a function of $x_{[bmim][PF6]}$, and are given in Figure 1C alongside the ideal α response in the [bmim][PF_6] + TFE mixture. As expected, α for neat TFE is significantly higher than that for neat [bmim][PF_6], and both are in good agreement with those reported earlier.[19] The α values of [bmim][PF_6] + TFE mixtures reveal a trend in α similar to that observed for E_T^N; however, the synergy in α is even more pronounced. This synergy persists for $x_{[bmim][PF6]}$ up to 0.9, emphasizing that even a minor addition of TFE to [bmim][PF_6] (or vice versa) leads to a striking increase in HBD acidity for the system. Comparing trends in π^*, E_T^N, and α values, it is clear that the synergy in E_T^N within the mixture arises from the exceptionally strong synergy in α, which overcomes a somewhat antagonistic trend in π^*. Accordingly, the [bmim][PF_6] + TFE system must possess exceptionally high HBD acidity and while solute−solvent interactions certainly contribute to these measurements, solvent−solvent interactions must be invoked to explain these unusual observations. The strong synergy in HBD acidity of the [bmim][PF_6] + TFE mixture combined with the fact that TFE has almost no HBA basicity (i.e., $\beta \approx 0$ for TFE) points to the significance of β estimated for [bmim][PF_6] + TFE mixtures given that (1) the anion is the predominant player in determining the IL's HBA basicity[39] and (2) the [PF_6]$^-$ anion is apparently necessary for the observation of synergy in E_T^N and α values (*vide infra*). ILs containing the [PF_6]$^-$ anion often have lower β values compared to other ILs.[39,40,47] The experimental β values within [bmim][PF_6] + TFE mixtures were obtained using eq 5 and are plotted along with the ideal additive values in Figure 1D. Our values of β in neat TFE and neat [bmim][PF_6] are again in accord with those reported earlier.[19,39,40] Interestingly, small amounts of [bmim][PF_6] added to TFE result in a sharp increase in the β value of the mixture. Similar to the observations for E_T^N and α, the β values of the mixture at all compositions are significantly higher than those predicted from simple additive considerations. Further, more synergism is observed in the IL-rich regime ($x_{[bmim][PF6]} > 0.6$). The mixture even possesses appreciable HBA basicity in the TFE-rich regime ($x_{[bmim][PF6]} \approx 0.1$). Since TFE has limited H-bond acceptor basicity, this behavior is consistent with stronger H-bonding of the probe molecule with the [PF_6]$^-$ anion in the presence of TFE as compared to neat [bmim][PF_6] to produce a synergistic polarity effect.

Betaine Dye Response in TFE Mixtures with Other ILs. The synergism expressed in terms of E_T^N, α, and β in the [bmim][PF_6] + TFE system is a very rare example of hyperpolarity. To the best of our knowledge, the only other publication reporting on empirical measures of polarity in mixtures of TFE with any IL is work from the Brennecke group,[19] involving [hmim][Tf_2N] and [hmim][OTf]. These authors established trends different from those observed for these same ILs with various organic solvents (acetonitrile, 2-butanone, or dichloromethane). In contrast to our results, while preferential solvation in their work can be attributed to Reichardt's dye forming strong hydrogen bonds with TFE, absolutely no synergism was observed in their $E_T(30)$ values. Closer inspection of their data reveals marginal or questionable synergism in α in the TFE-rich region of mixtures of TFE with [hmim][Tf_2N] or [hmim][OTf]. The trends in their reported π^* values in TFE mixtures with both ILs are similar to that observed in the current study. Due to the insignificant synergism observed in their work, Brennecke and co-workers soundly explain their trends on the basis of preferential interactions between the probes and a single component of the mixture. This distinction between our results and those of the

dx.doi.org/10.1021/jp210199s | J. Phys. Chem. B 2012, 116, 1360−1369

Brennecke group points to the importance of the nature of the anion, an aspect we will discuss next.

To clarify ion-dependent trends for IL mixtures with TFE, we measured the optical absorbance of betaine dye 30 in [hmim][PF_6], [bmim][Tf_2N], [bmim][BF_4], [hmim][BF_4], [omim][BF_4], and [bmpyrr][$B(CN)_4$], as well as their equimolar mixtures with TFE. Recall that E_T^N values showed prominent synergism for the equimolar mixture between [bmim][PF_6] and TFE. For ease of comparison, the estimated E_T^N values in neat ILs, as well as in their equimolar mixtures with TFE, are presented alongside that for [bmim][PF_6] (Figure 2). Three important outcomes can be garnered from

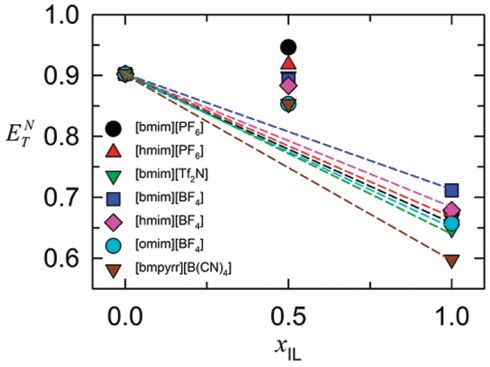

Figure 2. Variation in the E_T^N parameter measured in neat TFE, in various pure ILs, and for their equimolar mixtures with TFE. The dashed lines show the anticipated mole-fraction-weighted behavior indicative of ideal solvent mixing.

these results. First, in line with what has been reported in the literature, irrespective of anion choice, E_T^N values for imidazolium-based ILs all appear to be fairly similar but are higher than the corresponding E_T^N values for pyrrolidinium-based ILs.[39−45] Second, though the E_T^N values for neat ILs are significantly lower than the value for neat TFE, E_T^N values for equimolar mixtures with TFE lie closer to the value for neat TFE than for neat IL. Apart from pointing to a general deviation from ideal solvation in the mixture, this behavior suggests the presence of H-bonding interactions that are somewhat independent of the specific ions constituting the IL. Third, and most importantly, system synergism indicated by hyperpolarity (i.e., the observation of E_T^N values in the mixture exceeding those of neat TFE) is only seen for ILs containing the hexafluorophosphate ($[PF_6]^-$) anion. Again, we attribute this outcome in part to the lower HBA basicity of $[PF_6]^-$ -based ILs compared to other common ILs studied.[19,41,43,46−55]

Behavior of Fluorescence Probes within [bmim][PF_6] + TFE Mixtures. To gain deeper insight into the interactions present within [bmim][PF_6] + TFE mixtures, we included the study of three well-known fluorescent dipolarity probes: 2-(*p*-toluidino)naphthalene-6-sulfonate (TNS), 6-propionyl-2-(dimethylamino)naphthalene (PRODAN), and pyrene (Py). Fluorescence probes are well-suited for gathering information regarding complex systems owing to the high sensitivity and orthogonality of information inherent to fluorescence techniques.[56] TNS displays fluorescence emission maxima (λ_{max}^{em}) ranging from around 420−440 nm in low-polarity organic solvents to ca. 500 nm in water.[57] This behavior is due to the existence of two different excited states possessing distinct sensitivities to solvent polarity. In solvents of low polarity, the $\pi-\pi^*$ state is dominant as the first excited state is characterized by a nonplanar orientation of the two aromatic rings in the probe. The second excited state arises from an intramolecular electron transfer in the TNS molecule from the phenyl ring (donor) to the naphthalene ring (acceptor) and is highly sensitive to the solvent polarity. Similarly, the λ_{max}^{em} of PRODAN is highly sensitive to solvent polarity, ranging from ca. 392 nm in cyclohexane to 523 nm in water.[58,59] The polarity dependence of PRODAN fluorescence emission is attributed to an ICT excited state.[60] In this state, the carbonyl group intramolecularly gains electron density at the expense of the dimethylamino group, resulting in an increased molecular dipole moment. Figure 3A,B presents experimental and

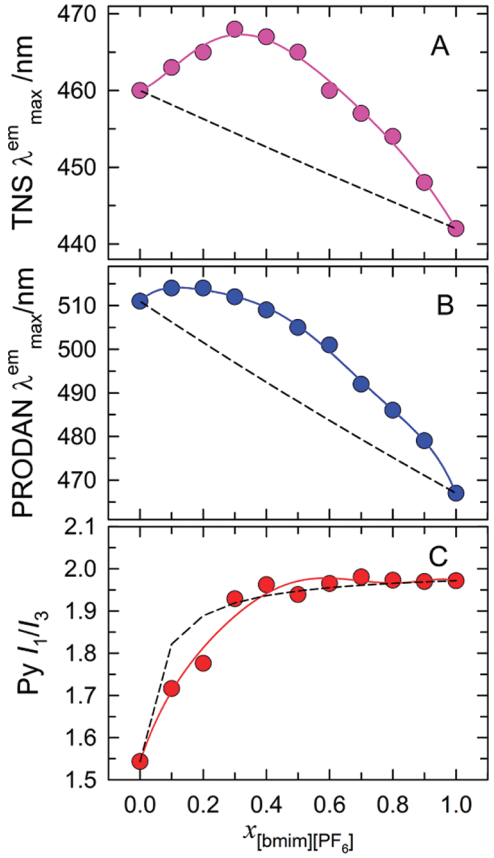

Figure 3. Variation in (A) TNS and (B) PRODAN λ_{max}^{em} values (both with an imprecision of 2 nm) and (C) the Py I_1/I_3 index with solvent composition in the [bmim][PF_6] + TFE system. All probes are present at 1 μM. Dashed profiles display the predicted behavior, and solid profiles give the response generated using the recovered parameters (Table 1) to Redlich−Kister best fits.

idealized λ_{max}^{em} values for TNS and PRODAN, respectively, in the [bmim][PF_6] + TFE system. Mole-fraction-weighted values were determined from reciprocal values of λ_{max}^{em} in order to express the emission along energy coordinates. Similarly to E_T^N, π^*, and α, both TNS and PRODAN showed higher λ_{max}^{em} values in neat TFE in comparison to neat [bmim][PF_6], in agreement with the higher dipolarity claimed for TFE. In line with the earlier E_T^N and α results, clear synergy is observed in the magnitude of λ_{max}^{em} up to 0.35 and 0.65 mol fractions of [bmim][PF_6] in mixtures with TFE for the probes PRODAN and TNS, respectively. The presence of functionalities on both TNS and PRODAN capable of participating in H-bonding alongside the excited-state electron/charge transfer is likely

dx.doi.org/10.1021/jp210199s | J. Phys. Chem. B 2012, 116, 1360−1369

Table 1. Recovered Parameters (A_j), Standard Deviations (σ), and Correlation Coefficients (r^2) for Fits of Different Experimental Solvatochromic Parameters (SP) Measured in [bmim][PF_6] + TFE to a Redlich–Kister-Type Polynomial Expansion (Equation 7)

SP	A_0	A_1	A_2	A_3	A_4	σ	r^2
E_T^N	0.6299	0.1752	0.2095	0.4814	1.2192	0.0059	0.9998
π^*	−0.2070	0.0816	−0.2382	−0.1016	0.4079	0.0274	0.6876
α	1.4736	0.3095	0.6121	1.0847	2.2703	0.0180	0.9967
β	0.3394	−0.1823	0.7733	−0.3241	−0.0629	0.0279	0.9943
TNS λ_{max}^{em}/nm	53.6794	−20.5452	4.7908	29.2671	−16.4831	5.3127	0.6492
PRODAN λ_{max}^{em}/nm	65.5193	−14.2964	−22.6223	23.1147	79.3868	4.1068	0.8991
Py I_1/I_3	0.8541	−0.5111	−0.3207	−0.0812	0.6831	0.1781	0.8537

responsible for this observation. The fact that TNS has a much more prominent synergy in its λ_{max}^{em} response (i.e., hyperpolarity) as compared to PRODAN further upholds this claim as the secondary amine present in TNS is capable of both HBD and HBA in addition to the HBA ability of its anionic sulfonate functionality. In contrast, PRODAN presents only the relatively weaker HBA sites within its tertiary amine and carboxyl functionalities.

The pyrene solvent polarity scale (Py I_1/I_3) is defined by the fluorescence intensity ratio of the first and third emission bands for pyrene, where I_1 is the intensity of the solvent-sensitive band arising from the $S_1(v = 0) \rightarrow S_0(v = 0)$ transition and I_3 corresponds to the solvent-insensitive $S_1(v = 0) \rightarrow S_0(v = 1)$ emissive transition.[61,62] The Py I_1/I_3 ratio increases with increasing solvent dipolarity and is a function of both the solvent dielectric (ε) and the refractive index (n) via the dielectric cross term, $f(\varepsilon, n^2)$. Experimentally measured and additive Py I_1/I_3 values are compared in the [bmim][PF_6] + TFE system in Figure 3C. As reported earlier, Py I_1/I_3 in neat [bmim][PF_6] is higher than in neat TFE.[29,31] This is most likely a manifestation of the fact that pyrene bears no functionality (heteroatoms) capable of involvement in H-bonding with the solubilizing milieu. Py I_1/I_3 systematically increases as [bmim][PF_6] is added to TFE, and interestingly, the experimental Py I_1/I_3 values in the [bmim][PF_6] + TFE mixture closely track the ideal, mole-fraction-averaged values calculated from eq 6.[63]

$$\left(\frac{I_1}{I_3}\right)_{cal} = \frac{(I_{1,[bmim][PF_6]} \times x_{[bmim][PF_6]}) + (I_{1,TFE} \times x_{TFE})}{(I_{3,[bmim][PF_6]} \times x_{[bmim][PF_6]}) + (I_{3,TFE} \times x_{TFE})} \quad (6)$$

Taken in context with the collective responses of the various other probes used to investigate the [bmim][PF_6] + TFE system here, it is easy to comprehend the well-behaved response of Py I_1/I_3, given that pyrene is devoid of functionality that could become involved in excited-state electron/charge transfer or H-bonding. We suggest that this makes pyrene an excellent choice for unbiased probing of general dipolarity within ILs. And yet, it is clear that pyrene is blind to specific solvent effects such as the solute–solvent and solvent–solvent H-bonding interactions present in the [bmim][PF_6] + TFE mixture which give rise to the distinctive synergy at the core of the "anomalous" optical probe responses seen here. We would also stress that the presence of such H-bonding interactions is not solely of academic interest. As later sections will substantiate, the unique organization that occurs in the [bmim][PF_6] + TFE system is also evidenced by probe-free techniques. More to the point, the locally enhanced polarity is not merely a spectroscopic peculiarity but also begs the stimulating question as to whether such systems might be put to good use synthetically, for example in the stabilization of highly polar reaction intermediates or transition states.

Modeling Probe Responses Using Redlich–Kister Polynomials. Empirical parameters such as those studied here are useful in correlating a wide range of physicochemical properties.[64] In turn, the reliable prediction of solvent parameters for mixtures based on a minimum number of experimental data provides a practical and expedient computational tool. In order to reveal the effect of solution composition on the various empirical parameters determined here, we applied the combined nearly ideal binary solvent/Redlich–Kister (CNIBS/R-K) equation to the experimental data for these parameters.[65] According to the CNIBS/R-K model, the empirical parameters (SP) in a binary solvent mixture at a constant temperature can be conveniently expressed as

$$SP_m = x_{[bmim][PF_6]}SP^0_{[bmim][PF_6]} + x_{TFE}SP^0_{TFE} + x_{[bmim][PF_6]}x_{TFE}\sum_{j=0}^{k} A_j(x_{[bmim][PF_6]} - x_{TFE})^j \quad (7)$$

where SP_m, $SP^0_{[bmin][PF_6]}$, and SP^0_{TFE} are parameters determined in the [bmim][PF_6] + TFE mixture, neat [bmim][PF_6], and neat TFE, respectively. In eq 7, A_j and j represent the equation coefficients and the degree of the polynomial expansion, respectively. In practice, the numerical value of j is increased integer-wise and regression analysis performed to fit the experimental data to polynomials of increasing order until a sufficiently accurate mathematical description of the experimental data is reached. The results of fittings to the CNIBS/R-K model (with $j = 4$) are compiled in Table 1 and are shown graphically as dashed profiles in Figures 1 and 3 for each of the following parameters: E_T^N, π^*, α, β, TNS λ_{max}^{em}, PRODAN λ_{max}^{em}, and Py I_1/I_3. The fact that a value of $j = 4$ was required to obtain a reasonable fit to these data further highlights the complexity associated with the [bmim][PF_6] + TFE mixture.

FTIR Spectroscopy of [bmim][PF_6] + TFE Mixtures. In order to examine the H-bonding interactions arising within the [bmim][PF_6] + TFE mixture in a nonintrusive manner (i.e., in the absence of an extrinsic molecular probe), we collected FTIR absorbance spectra of the mixture at representative compositions ranging from neat [bmim][PF_6] to pure TFE (Figure 4). The FTIR spectrum collected for [bmim][PF_6] was completely in line with previously published spectra[66] and was thusly assigned as follows: 1170 cm^{-1}, 1340 cm^{-1}, and 1387

dx.doi.org/10.1021/jp210199s | J. Phys. Chem. B 2012, 116, 1360–1369

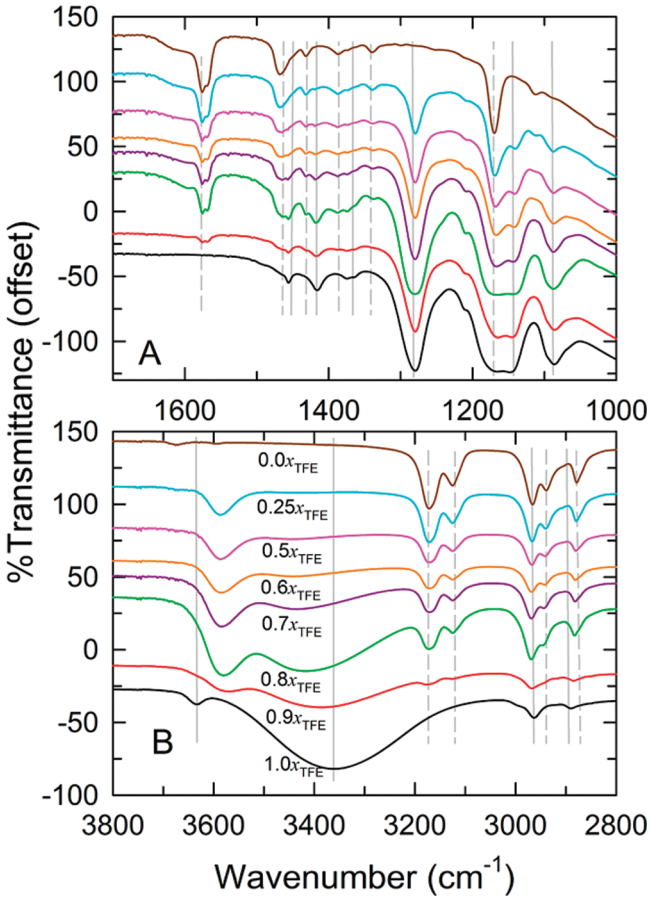

Figure 4. FTIR spectra of representative [bmim][PF_6] + TFE mixtures in the (A) 1700−1000 cm^{-1} and (B) 3800−2800 cm^{-1} windows. Data from 2800−1700 cm^{-1} are not included due to the absence of IR features in this region. Solid and dashed vertical lines denote IR assignments for TFE and [bmim][PF_6] components, respectively.

cm^{-1} are attributed to CH_3(N), CH_2(N), and in-plane asymmetric ring stretch, respectively; 1432 cm^{-1} is assigned to an in-plane asymmetric ring stretch and CH_3(N) stretch; the 1468 cm^{-1} peak indicates a CH_3(N) HCH bend; 1576 cm^{-1} is an also assigned to an in-plane asymmetric ring stretch; 2878 cm^{-1} is a CH_2C(N) HCH symmetric stretch and terminal CH_3 HCH symmetric stretch; 2939 cm^{-1} is a CH_3(N) HCH symmetric stretch; 2966 cm^{-1} is a propyl HCH asymmetric stretch; 3125 cm^{-1} is a NC(H)N CH stretch; and 3172 cm^{-1} is a ring HCCH asymmetric stretch. A close examination of these data reveals that there is no perceptible shift in any of the major IR peaks for [bmim][PF_6] upon addition of TFE. Most noteworthy is the lack of shift for the NC(H)N CH stretch appearing near 3125 cm^{-1}, as this C-2 hydrogen is reportedly the most acidic and largely responsible for the HBD acidity of imidazolium-based ILs.[39] The lack of noticeable shift in this IR peak indicates the absence of significant change in H-bonding involving the C-2 proton of [bmim]$^+$ as TFE is added to [bmim][PF_6]. Since TFE displays very limited HBA basicity, the NA probe used to obtain the HBA basicity parameter (β) apparently preferentially H-bonds with [PF_6]$^-$ in the mixture. The moderate synergism in β may therefore be due to the disruption in electrostatic and/or H-bonding attractions between [bmim]$^+$ and [PF_6]$^-$ resulting from the addition of TFE, to liberate a [PF_6]$^-$ population characterized by enhanced HBA basicity relative to that in neat [bmim][PF_6]. The proposed loss in interionic electrostatic attraction and H-bonding in [bmim][PF_6] mixtures containing TFE is further highlighted by measurements of the dynamic viscosity and density (*vide infra*).

In distinction to the stationary [bmim][PF_6] peaks, the FTIR peaks associated with TFE do show noteworthy changes as [bmim][PF_6] is added. While the nonhydroxyl group vibrational assignments at 1087, 1150, 1165, 1280, 1374, 1416, 1455, 2889, and 2962 cm^{-1} generally show no appreciable changes, peaks for vibrations associated with the O−H group at 3363 and 3633 cm^{-1} for TFE undergo significant changes as [bmim][PF_6] is added (Figure 4B). For TFE, three overlapping absorption bands dominate the O−H stretching region and are rationalized in terms of various H-bonded structures.[67,68] In neat TFE, the O−H stretch for "introverted" monomeric TFE, intramolecularly H-bonded between the OH group and fluorine of the CF_3 group, appears at the highest energy (i.e., the band at 3633 cm^{-1}).[69] Dimeric TFE structures are associated with a band at ca. 3500 cm^{-1}, and polymeric structures corresponding to multimers with extended H-bonding are assigned to the broad band centered at 3363 cm^{-1}.[69] An important aspect of these FTIR data is that as [bmim][PF_6] is added to TFE, the position of the O−H stretch assigned to TFE multimers immediately shifts to higher frequency accompanied by a remarkable diminution in intensity, becoming virtually nonexistent by $x_{[bmim][PF6]}$ = 0.5. This clearly points to a dramatic disintegration of the extended H-bonding network involving TFE multimers.

At the same time, when as little as a 0.1 mol fraction of [bmim][PF_6] is added to TFE, the ν_{OH} band for *gauche*-TFE at 3633 cm^{-1} abruptly red shifts to 3590 cm^{-1} which we tentatively assign to an O−H stretch for species no longer involved in intramolecular H-bonding but ones now free to "mingle" intermolecularly. This is most likely due to the CF_3 groups of TFE preferentially interacting with the butyl group of [bmim]$^+$, as suggested by recent NMR studies from the Sun group[70] which advocate a disruption in [PF_6]$^-$/[bmim]$^+$ butyl chain H-bonding within similar mixtures.[71] If true, the upshot would be liberated OH groups now available to act as stronger HBDs toward polarity-sensitive dyes, a consequence compatible with the hyperpolarity witnessed for the E_T^N and α values in the [bmim][PF_6] + TFE mixture. Further, and perhaps most importantly, earlier NMR spectroscopy studies revealed that hyper anion preference aggregates (HAPAs) are formed in [bmim][PF_6] + TFE mixtures; i.e., [PF_6−bmim−PF_6]$^-$ is preferred over [bmim−PF_6−bmim]$^+$.[70] Similarly charged clusters were suggested to form in [bmim][PF_6] by the Watanabe group on the basis of fast atom bombardment-mass spectrometry (FAB-MS) spectra.[72] HAPA discrimination consequently leads to more free [bmim]$^+$ in solution, also capable of acting as a HBD toward solutes (or molecular probes), especially considering the fact that TFE has essentially null HBA basicity and is thus unlikely to engage [bmim]$^+$ in H-bonding. This emancipated [bmim]$^+$ surely contributes to the synergism observed in E_T^N, α, and λ_{max}^{em} (TNS and PRODAN) values determined for [bmim][PF_6] + TFE.

Dynamic Viscosity and Density Measurements of [bmim][PF_6] + TFE. Dynamic viscosity and density measurements afforded auxiliary evidence to support the notion of disruption in both Coulombic attraction and intermolecular H-bonding between [bmim]$^+$ and [PF_6]$^-$ upon TFE addition. Experimental dynamic viscosities and the reciprocal densities of

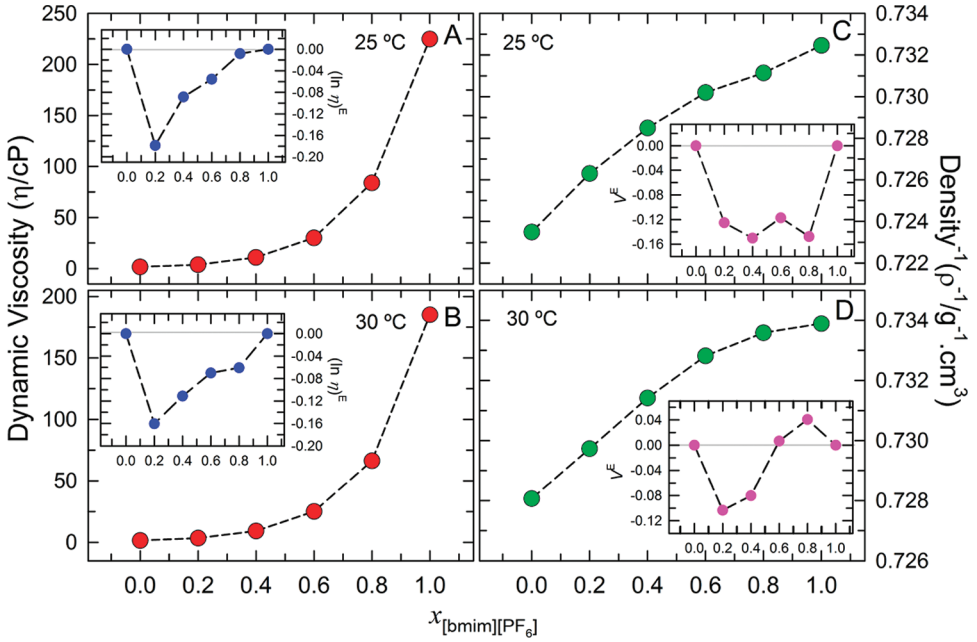

Figure 5. Composition-dependent dynamic viscosities (η, ±0.5%) at (A) 25 °C and (B) 30 °C and reciprocal densities (ρ^{-1}, ± 0.1%) at (C) 25 °C and (D) 30 °C for the [bmim][PF_6] + TFE mixture. The corresponding insets show excess logarithmic viscosity [$(\ln \eta)^E$] and excess molar volume (V^E). The dashed curves are simply to guide the eye.

the [bmim][PF_6] + TFE mixtures at 25 and 30 °C are presented in Figure 5, where the respective insets display excess logarithmic viscosity [$(\ln \eta)^E$] and excess molar volume (V^E). Negative $(\ln \eta)^E$ values across the entire composition range clearly imply that the observed viscosity for the mixture is well below the prediction. Additionally, the inverted funnel shape of $(\ln \eta)^E$ for the [bmim][PF_6] + TFE system may reflect overlapping effects (namely, disruption in electrostatic attraction in the [bmim][PF_6]-rich region on the one hand and a breakup of intermolecular H-bonding on the other, particularly in the TFE-rich regime) as well as a size mismatch between [bmim][PF_6] and TFE. However, the latter effect is likely of lesser importance given the fact that $(\ln \eta)^E$ for various [bmim][PF_6] + PEG mixtures actually displayed "hyper-viscosity".[73] Although disruption in electrostatic attraction and/or H-bonding is not expected to exert as dramatic an impact on density, the negative V^E at 25 °C may be due to the formation of HAPAs, especially since it becomes less pronounced at 30 °C (i.e., elevated temperature should lead to a reduction in aggregation).[70] Besides, the absolute values of V^E at 25 °C for [bmim][PF_6] + TFE mixtures are considerably smaller ($V^E \approx -0.15$ cm^3 mol^{-1}) than those reported for near-equimolar [bmim][PF_6] + PEG mixtures where extensive H-bonding between [bmim][PF_6] and PEG have been invoked: $V^E \approx -0.80$, -2.5, -3.6, and -5.0 cm^3 mol^{-1} for 1:1 [bmim][PF_6]/PEG for 200, 400, 600, and 1000 Da PEG, respectively.[74,75]

CONCLUSIONS

Distinct solute−solvent and solvent−solvent interactions within the [bmim][PF_6] + TFE mixed solvent system are amply manifested by responses from solvatochromic optical probes, as well as independent FTIR spectroscopy, viscometry, and density measurements. Taken in sum, our data suggest a number of features for the [bmim][PF_6] + TFE system: (i) extended H-bonding involving multimers of TFE is disrupted with intramolecular H-bonding in TFE involving fluorine significantly weakened; (ii) Coulombic attraction as well as any H-bonding between bmim$^+$ and PF_6^- is considerably reduced in the mixture; (iii) HAPAs are possibly formed resulting in "free" [bmim]$^+$; and (iv) no appreciable H-bonding is seen between [bmim]$^+$ and TFE. Increasing levels of [bmim][PF_6] manifest in disrupted intramolecular H-bonding in monomeric TFE as well as breaking up polymeric H-bonded TFE networks, making TFE more "extroverted". Similarly, "free" [bmim]$^+$ arising from addition of TFE to [bmim][PF_6] also contributes to the manifestation of hyperpolarity, as illustrated in the remarkably elevated E_T^N and α values. This synergy is also reflected in the responses from fluorescent probes capable of contributing to H-bond formation, especially those with HBA character. Although more speculative, a population of HAPAs giving rise to synergistically elevated β values in the [bmim][PF_6] + TFE mixture appears to be operative. Results gained via noninvasive techniques that do not require a probe *per se*, including FTIR, dynamic viscosity, and density, readily complement our collective probe study. Overall, the complex interactions within the [bmim][PF_6] + TFE mixture are a manifestation of a complex interplay of both general (Coulombic, van der Waals attractive, and short-range repulsive) and specific (H-bonding, HAPA formation) interactions present in this system in addition to *gauche*−*trans* TFE conformational dynamics and oligomerization. The emergent features (hyperpolarity) and inherent complexity suggest a clear necessity for further spectroscopic and rheological analysis as well as molecular dynamics and *ab initio* quantum chemical studies, a door we hope is opened in the present work.

AUTHOR INFORMATION

Corresponding Author

*E-mail: bakershei@missouri.edu (S.N.B.), bakergar@missouri.edu (G.A.B.), pandeys@missouri.edu (Siddharth Pandey),

sipandey@chemistry.iitd.ac.in (Siddharth Pandey). Phone: +1-573-882-3691 (S.N.B.), +1-573-882-1811 (G.A.B.), +1-573-214-1311 (Siddharth Pandey), +91-11-26596503 (Siddharth Pandey).

■ ACKNOWLEDGMENTS

This work was generously supported by the Department of Science and Technology, India, through Grant SR/S1/PC-16/2008 to Siddharth Pandey. S.T. would like to thank UGC, India, for a fellowship.

■ REFERENCES

(1) Wasserscheid, P.; Welton, T. *Ionic Liquids in Synthesis*; Wiley-VCH: New York, 2003.
(2) Berthod, A.; He, L.; Armstrong, D. W. *Chromatographia* **2001**, *53*, 63.
(3) Seki, S.; Kobayashi, Y.; Miyashiro, H.; Ohno, Y.; Usami, A.; Mita, Y.; Watanabe, M.; Terada, N. *Chem. Commun.* **2006**, 544.
(4) Mazille, F.; Fei, Z.; Kuang, D.; Zhao, D.; Zakeeruddin, S. M.; Grätzel, M.; Dyson, P. J. *Inorg. Chem.* **2006**, *45*, 1585.
(5) Ye, C.; Liu, W.; Chen, Y.; Yu, L. *Chem. Commun.* **2001**, 2244.
(6) Pandey, S.; Fletcher, K. A.; Baker, S. N.; Baker, G. A. *Analyst* **2004**, *129*, 569.
(7) Fletcher, K. A.; Pandey, S. *J. Phys. Chem. B* **2003**, *107*, 13532.
(8) *Solvents and Solvent Effects in Organic Chemistry*; Reichardt, C., Ed.; Wiley-VCH: Weinheim, Germany, 2003.
(9) Shiraki, K.; Nishikawa, K.; Goto, Y. *J. Mol. Biol.* **1995**, *245*, 180.
(10) Lu, H.; Buck, M.; Radford, S. E.; Dobson, C. M. *J. Mol. Biol.* **1997**, *265*, 112.
(11) Buck, M. *Q. Rev. Biophys.* **1998**, *31*, 297.
(12) Becker, J. Y.; Smart, B. E.; Fukunaga, T. *J. Org. Chem.* **1988**, *53*, 5714.
(13) Bégué, J.-P.; Bonnet-Delpon, D.; Crousse, B. *Synlett* **2004**, *1*, 18.
(14) Shuklov, I. A.; Dubrovina, N. V.; Börner, A. *Synthesis* **2007**, 2925.
(15) Ravikumar, K. S.; Kesavan, V.; Crousse, B.; Bonnet-Delpon, D.; Bégué, J.-P. *Org. Synth.* **2003**, *80*, 184.
(16) Castagnola, M.; Cassiano, L.; Messana, I.; Paci, M.; Rossetti, D. V.; Giardina, B. *J. Chromatogr., A* **1996**, *735*, 271.
(17) Siegemund, G.; Schwertfeger, W.; Feiring, A.; Smart, B.; Behr, F.; Vogel, H.; McKusick, B. Fluorine Compounds, Organic. *Ullmann's Encyclopedia of Industrial Chemistry*; John Wiley & Sons: New York, 2007.
(18) Moïse, J.-C.; Mutelet, F.; Juabert, J.-N.; Grubbs, L. M.; Acree, W. E. Jr.; Baker, G. A. *J. Chem. Eng. Data* **2011**, *56*, 3106.
(19) Mellein, B. R.; Aki, S. N. V. K.; Ladewski, R. L.; Brennecke, J. F. *J. Phys. Chem. B* **2007**, *111*, 131.
(20) Mutelet, F.; Revelli, A. L.; Jaubert, J. N.; Sprunger, L. M.; Acree, W. E. Jr.; Baker, G. A. *J. Chem. Eng. Data* **2010**, *55*, 234.
(21) François, Y.; Zhang, K.; Varenne, A.; Gareil, P. *Anal. Chim. Acta* **2006**, *562*, 164.
(22) Kang, J. E.; Lee, J. S.; Kim, D. S.; Lee, S. D.; Lee, H.; Kim, H. S.; Cheong, M. *J. Catal.* **2009**, *262*, 177.
(23) Currás, M. R.; Gomes, M. F. C.; Husson, P.; Padua, A. A. H.; Garcia, J. *J. Chem. Eng. Data* **2010**, *55*, 5504.
(24) Terayama, Y.; Kikuchi, M.; Kobayashi, M.; Takahara, A. *Macromolecules* **2011**, *44*, 104.
(25) Bini, R.; Chiappe, C.; Pieraccini, D.; Piccioli, P.; Pomelli, C. S. *Tetrahedron Lett.* **2005**, *46*, 6675.
(26) Burrell, A. K.; Del Sesto, R. E.; Baker, S. N.; McCleskey, T. M.; Baker, G. A. *Green Chem.* **2007**, *9*, 449.
(27) Page, P. M.; McCarty, T. A.; Baker, G. A.; Baker, S. N.; Bright, F. V. *Langmuir* **2007**, *23*, 843.
(28) Marcus, Y. *Chem. Soc. Rev.* **1993**, *22*, 409.
(29) Sarkar, A.; Trivedi, S.; Baker, G. A.; Pandey, S. *J. Phys. Chem. B* **2008**, *112*, 14927.
(30) Sarkar, A.; Trivedi, S.; Pandey, S. *J. Phys. Chem. B* **2008**, *112*, 9042.
(31) Sarkar, A.; Trivedi, S.; Pandey, S. *J. Phys. Chem. B* **2009**, *113*, 7606.
(32) *Solvatochromism*; Suppan, P., Ghoneim, N., Eds.; Royal Society of Chemistry: Cambridge, U.K., 1997.
(33) Marcus, Y. *Solvent Mixtures: Properties and Selective Solvation*; Marcel Dekker: New York, 2002 and references cited therein.
(34) Kamlet, M. J.; Abboud, J. L.; Taft, R. W. *J. Am. Chem. Soc.* **1977**, *99*, 6027.
(35) Taft, R. W.; Kamlet, M. J. *J. Am. Chem. Soc.* **1976**, *98*, 2886.
(36) Kamlet, M. J.; Taft, R. W. *J. Am. Chem. Soc.* **1976**, *98*, 377.
(37) Kamlet, M. J.; Abboud, J. L.; Abraham, M. H.; Taft, R. W. *J. Org. Chem.* **1983**, *48*, 2877.
(38) Fletcher, K. A.; Storey, I. K.; Hendricks, A. E.; Pandey, S.; Pandey, S. *Green Chem.* **2001**, *3*, 210.
(39) Crowhurst, L.; Mawdsley, P. R.; Perez-Arlandis, J. M.; Salter, P. A.; Welton, T. *Phys. Chem. Chem. Phys.* **2003**, *5*, 2790.
(40) Muldoon, M. J.; Gordon, C. M.; Dunkin, I. R. *J. Chem. Soc., Perkins Trans. 2* **2001**, *4*, 433.
(41) Baker, S. N.; Baker, G. A.; Bright, F. V. *Green Chem.* **2002**, *4*, 165.
(42) Fletcher, K. A.; Pandey, S. *Proc. Electrochem. Soc.* **2002**, *19*, 244.
(43) Fletcher, K. A.; Baker, S. N.; Baker, G. A.; Pandey, S. *New J. Chem.* **2003**, *27*, 1706.
(44) Reichardt, C. *Green Chem.* **2005**, *7*, 339.
(45) Bartsch, R. A.; Dzyuba, S. V. In *Ionic Liquids as Green Solvents—Progress and Prospects*; American Chemical Society: Washington, DC, 2003; pp 289–299.
(46) Crowhurst, L.; Falcone, R.; Lancaster, N. L.; Llopis-Mestre, V.; Welton, T. *J. Org. Chem.* **2006**, *71*, 8847.
(47) Lungwitz, R.; Strehmel, V.; Spange, S. *New J. Chem.* **2010**, *34*, 1135.
(48) Ab Rani, M. A.; Brant, A.; Crowhurst, L.; Dolan, A.; Lui, M.; Hassan, N. H.; Hallett, J. P.; Hunt, P. A.; Niedermeyer, H.; Perez-Arlandis, J. M.; Schrems, M.; Welton, T.; Wildinga, R. *Phys. Chem. Chem. Phys.* **2011**, *13*, 16831.
(49) Chiappe, C.; Pomelli, C. S.; Rajamani, S. *J. Phys. Chem. B* **2011**, *115*, 9653.
(50) Palgunadi, J.; Hong, S. Y.; Lee, J. K.; Lee, H.; Lee, S. D.; Cheong, M.; Kim, H. S. *J. Phys. Chem. B* **2011**, *115*, 1067.
(51) Oehlke, A.; Hofmann, K.; Spange, S. *New J. Chem.* **2006**, *30*, 533.
(52) Wu, Y.; Sasaki, T.; Kazushi, K.; Seo, T.; Sakurai, K. *J. Phys. Chem. B* **2008**, *112*, 7536.
(53) Lee, J. M.; Ruckes, S.; Prausnitz, J. M. *J. Phys. Chem. B* **2008**, *112*, 1473.
(54) Strehmel, V.; Lungwitz, R.; Rexhausena, H.; Spange, S. *New J. Chem.* **2010**, *34*, 2125.
(55) Jeličić, A.; García, N.; Löhmannsröben, H. S.; Beuermann, S. *Macromolecules* **2009**, *42*, 8801.
(56) Acree, W. E., Jr. Absorption and Luminescence Probes. In *Encyclopedia of Analytical Chemistry: Theory and Instrumentation*; Meyer, R. A., Ed.; John Wiley & Sons, Ltd.: Chichester, U.K., 2000 and references cited therein.
(57) McClure, W. O.; Edelman, G. M. *Biochemistry* **1966**, *5*, 1908.
(58) Sun, S.; Heitz, M. P.; Bruckenstein, S.; Perez, S. A.; Colón, L. A.; Bright, F. V. *Appl. Spectrosc.* **1997**, *51*, 1316 and references therein.
(59) Weber, G.; Farris, F. J. *Biochemistry* **1979**, *18*, 3075.
(60) Everett, R. K.; Nguyen, H. A. A.; Abelt, C. J. *J. Phys. Chem. A* **2010**, *114*, 4946.
(61) Dong, D. C.; Winnik, M. A. *Can. J. Chem.* **1984**, *62*, 2560.
(62) Karpovich, D. S.; Blanchard, G. J. *J. Phys. Chem.* **1995**, *99*, 3951.
(63) Acree, W. E. Jr.; Wilkins, D. C.; Tucker, S. A.; Griffin, J. M.; Powell, J. R. *J. Phys. Chem.* **1994**, *98*, 2537.
(64) Kool, E. T.; Breslow, R. *J. Am. Chem. Soc.* **1988**, *110*, 1596.
(65) Redlich, O. J.; Kister, A. T. *Ind. Eng. Chem.* **1948**, *40*, 345.
(66) Talaty, E. R.; Raja, S.; Storhaug, V. J.; Dölle, A.; Carper, W. R. *J. Phys. Chem. B* **2004**, *108*, 13177.
(67) Blainey, P. C.; Reid, P. J. *Spectrochim. Acta* **2001**, *57A*, 2763.
(68) Coburn, W. C.; Grunwald, E. *J. Am. Chem. Soc.* **1958**, *80*, 1318.

(69) Perttila, M. *Spectrochim. Acta* **1979**, *35A*, 585.
(70) Hsu, W. Y.; Tai, C. C.; Su, W. L.; Chang, C. H.; Wang, S. P.; Sun, I. W. *Inorg. Chim. Acta* **2008**, *361*, 1281.
(71) Carper, W. R.; Wahlbeck, P. G.; Antony, J. H.; Mertens, A.; Dölle, A.; Wasserscheid, P. *Anal. Bioanal. Chem.* **2004**, *378*, 1548.
(72) Tokuda, H.; Hayamizu, K.; Ishii, K.; Susan, Md. A. B. H.; Wantanabe, M. *J. Phys. Chem. B* **2004**, *108*, 16593.
(73) Trivedi, S.; Pandey, S. *J. Phys. Chem. B* **2011**, *115*, 7405.
(74) Trivedi, S.; Pandey, S. *Indian J. Chem.* **2010**, *49A*, 731.
(75) Trivedi, S.; Pandey, S. *J. Chem. Eng. Data* **2011**, *56*, 2168.